

EUROPEAN LABORATORY FOR PARTICLE PHYSICS (CERN)

CERN-EP/99-035

1st March 1999

Measurement of W^- pair production in e^+e^- collisions at 183 GeV

The ALEPH Collaboration

Abstract

The production of W^+W^- pairs is analysed in a data sample collected by ALEPH at a mean centre-of-mass energy of 182.7 GeV, corresponding to an integrated luminosity of 57 pb^{-1} . Cross sections are given for different topologies of W^- decays into leptons or hadrons. Under Standard Model assumptions for the W^- pair production and decay, the W^- pair cross section is measured to be $15.57 \pm 0.62 \text{ (stat.)} \pm 0.29 \text{ (syst.) pb}$. Using also the W^- pair data samples collected by ALEPH at lower centre-of-mass energies, the decay branching ratio of the W^- boson into hadrons is measured to be $B(W^- \rightarrow \text{hadrons}) = 68.93 \pm 1.21 \text{ (stat.)} \pm 0.51 \text{ (syst.)\%}$, allowing a determination of the CKM matrix element $|V_{cs}| = 1.043 \pm 0.058 \text{ (stat.)} \pm 0.026 \text{ (syst.)}$. The agreement of the cross sections with the Standard Model prediction allows a limit to be set on the W^- decay rate to undetectable final states.

(to be Submitted to Physics Letters B)

The ALEPH Collaboration

R. Barate, D. Decamp, P. Ghez, C. Goy, S. Jezequel, J.-P. Lees, F. Martin, E. Merle, M.-N. Minard, B. Pietrzyk

Laboratoire de Physique des Particules (LAPP), IN²P³-CNRS, F-74019 Annecy-le-Vieux Cedex, France

R. Alemany, M. P. Casado, M. Chmeissani, J. M. Crespo, E. Fernandez, M. Fernandez-Bosman, L. Garrido,¹⁵ E. Grauges, A. Juste, M. Martinez, G. Merino, R. Miquel, L. Mir, P. Morawitz, A. Pacheco, I. C. Park, I. Riu

Institut de Física d'Altes Energies, Universitat Autònoma de Barcelona, 08193 Bellaterra (Barcelona), E-Spain⁷

A. Colaleo, D. Creanza, M. De Palma, G. Gelao, G. Iaselli, G. Maggi, M. Maggi, S. Nuzzo, A. Ranieri, G. Raso, F. Ruggieri, G. Selvaggi, L. Silvestris, P. Tempesta, A. Tricomì,³ G. Zito

Dipartimento di Fisica, INFN Sezione di Bari, I-70126 Bari, Italy

X. Huang, J. Lin, Q. Ouyang, T. Wang, Y. Xie, R. Xu, S. Xue, J. Zhang, L. Zhang, W. Zhao

Institute of High-Energy Physics, Academia Sinica, Beijing, The People's Republic of China⁸

D. Abbaneo, U. Becker,¹⁹ G. Boix,⁶ M. Cattaneo, V. Ciulli, G. Dissertori, H. Drevermann, R. W. Forty, M. Frank, F. Gianotti, A. W. Haldy, J. B. Hansen, J. Harvey, P. Janot, B. Jost, I. Lehraus, O. Leroy, C. Loomis, P. Maley, P. Mato, A. Merten, A. Moutoussi, F. Ranzard, L. Rolandi, D. Rousseau, D. Schlatter, M. Schmitt,²⁰ O. Schneider,²³ W. Tejessy, F. Teubert, I. Tomalin, E. Tourneer, M. Vreeswijk, A. E. Wright

European Laboratory for Particle Physics (CERN), CH-1211 Geneva 23, Switzerland

Z. Ajlouni, F. Badaud, G. Chazelle, O. Deschamps, S. Dessagne, A. Falvard, C. Ferdi, P. Gay, C. Guicheney, P. Henrard, J. Jousset, B. Michel, S. Monteil, J.-C. Montret, D. Pallin, P. Perret, F. Podlyski

Laboratoire de Physique Corpusculaire, Université Blaise Pascal, IN²P³-CNRS, Clermont-Ferrand, F-63177 Aubière, France

J. D. Hansen, J. R. Hansen, P. H. Hansen, B. S. Nilsson, B. Rensch, A. W. Sanner

Niels Bohr Institute, 2100 Copenhagen, DK-Denmark⁹

G. Daskalakis, A. Kyriakis, C. Markou, E. Simopoulou, A. Vayaki

Nuclear Research Center Demokritos (NRC), GR-15310 Attiki, Greece

A. Blondel, J.-C. Brient, F. Machefert, A. Rouge, M. Swynghedauw, R. Tanaka, A. Valassi,¹² H. Videau

Laboratoire de Physique Nucléaire et des Hautes Energies, Ecole Polytechnique, IN²P³-CNRS, F-91128 Palaiseau Cedex, France

E. Focardi, G. Parrini, K. Zachariadou

Dipartimento di Fisica, Università di Firenze, INFN Sezione di Firenze, I-50125 Firenze, Italy

R. Cavanaugh, M. Corden, C. Georgiopoulos

Supercomputer Computations Research Institute, Florida State University, Tallahassee, FL 32306-4052, USA^{13;14}

A. Antonelli, G. Bencivenni, G. Bologna,⁴ F. Bossi, P. Campana, G. Capon, F. Cerutti, V. Chiarella, P. Laurelli, G. Mannocchi,⁵ F. Murtas, G. P. Murtas, L. Passalacqua, M. Pepe-Aliarelli¹

Laboratori Nazionali dell'INFN (LNF-INFN), I-00044 Frascati, Italy

M. Chalmers, L. Curtis, J. G. Lynch, P. Negus, V. O'Shea, B. Raaven, C. Raine, D. Smith, P. Teixeira-

Dias, A. S. Thompson, J. J. Ward

Department of Physics and Astronomy, University of Glasgow, Glasgow G12 8QQ, United Kingdom¹⁰
O. Buchmüller, S. Dhamotharan, C. Geweniger, P. Hanke, G. Hansper, V. Hepp, E. E. Kluge, A. Putzer,
J. Sommer, K. Tittel, S. Wemer,¹⁹ M. Wunsch

Institut für Hochenergiephysik, Universität Heidelberg, D-69120 Heidelberg, Germany¹⁶

R. Beuselinck, D. M. Binnie, W. Cameron, P. J. Doman,¹ M. Girone, S. Goodson, N. Marinelli, E. B. Martin,
J. Nash, J. Nowell, A. Sciaba, J. K. Sedgbeer, P. Spagnolo, E. Thomson, M. D. Williams

Department of Physics, Imperial College, London SW 7 2BZ, United Kingdom¹⁰

V. M. Ghete, P. Girtler, E. Kneringer, D. Kuhn, G. Rudolph

Institut für Experimentalphysik, Universität Innsbruck, A-6020 Innsbruck, Austria¹⁸

A. P. Betteridge, C. K. Bowdery, P. G. Buck, P. Colrain, G. Crawford, G. Ellis, A. J. Finch, F. Foster,
G. Hughes, R. W. L. Jones, N. A. Robertson, M. I. Williams

Department of Physics, University of Lancaster, Lancaster LA1 4YB, United Kingdom¹⁰

P. van Gemeren, I. Gehl, F. Holdorfer, C. Homann, K. Jakobs, K. Kleinknecht, M. Kröcker, H.-
A. Numberger, G. Quast, B. Renk, E. Rohne, H.-G. Sander, S. Schmeling, H. Wachsmuth, C. Zeitnitz,
T. Ziegler

Institut für Physik, Universität Mainz, D-55099 Mainz, Germany¹⁶

J. J. Aubert, C. Bouchouk, A. Bonissent, J. Carr,¹ P. Coyle, A. Ealet, D. Fouchez, F. Mutsch, P. Payre,
M. Talby, M. Thulasidas, A. Tilquin

Centre de Physique des Particules, Faculté des Sciences de Luminy, IN²P³-CNRS, F-13288 Marseille,
France

M. Aleppo, M. Antonelli, F. Ragusa

Dipartimento di Fisica, Università di Milano e INFN Sezione di Milano, I-20133 Milano, Italy.

R. Berlich, V. Buscher, H. Dietl, G. Ganis, K. Huttmann, G. Lutjens, C. Mannert, W. Manter,
H.-G. Møser, S. Schael, R. Settles, H. Seywerd, H. Stenzel, W. Wiedenmann, G. Wolf

Max-Planck-Institut für Physik, Werner-Heisenberg-Institut, D-80805 München, Germany¹⁶

P. Azzurri, J. Boucrot, O. Callot, S. Chen, M. Davier, L. Duot, J.-F. Girivaz, Ph. Heusse,
A. Jacholkowska, M. Kado, J. Lefrançois, L. Serin, J.-J. Veillet, I. Videau,¹ J.-B. de Vivie de Regie,
D. Zerwas

Laboratoire de l'Accélérateur Linéaire, Université de Paris-Sud, IN²P³-CNRS, F-91898 Orsay Cedex,
France

G. Bagliesi, S. Bettarini, T. Boccali, C. Bozzi,²⁴ G. Calderini, R. Dell'Oso, I. Ferrante, A. Giassi,
A. Gregorio, F. Ligabue, A. Lusiani, P. S. Marrocchesi, A. Messineo, F. Palla, G. Rizzo, G. Sanguinetti,
G. Sguazzoni, R. Tenchini, C. Vannini, A. Venturi, P. G. Verdini

Dipartimento di Fisica dell'Università, INFN Sezione di Pisa, e Scuola Normale Superiore, I-56010
Pisa, Italy

G. A. Blair, J. Coles, G. Cowan, M. G. Green, D. E. Hutchcroft, L. T. Jones, T. Medcalf, J. A. Strong,
J. H. von Wimmersperg-Toeller

Department of Physics, Royal Holloway & Bedford New College, University of London, Surrey TW 20
0EX, United Kingdom¹⁰

D. R. Botterill, R. W. Clift, T. R. Edgecock, P. R. Norton, J. C. Thompson

Particle Physics Dept., Rutherford Appleton Laboratory, Chilton, Didcot, Oxon OX11 0QX, United
Kingdom¹⁰

B. Bouché-Devaux, P. Colas, B. Fabbro, G. Faif, E. Lancon, M.-C. Lemaire, E. Locci, P. Perez,
H. Przysiezniak, J. Rander, J.-F. Renardy, A. Rosowsky, A. Trabelsi,²¹ B. Tuchming, B. Vallage

CEA, DAPNIA/Service de Physique des Particules, CE-Saclay, F-91191 Gif-sur-Yvette Cedex,
France¹⁷

S. N. Black, J. H. Dann, H. Y. Kim, N. Konstantinidis, A. M. Litke, M. A. McNeil, G. Taylor

Institute for Particle Physics, University of California at Santa Cruz, Santa Cruz, CA 95064, USA²²

C.N. Booth, S. Cartwright, F. Combley, P.N. Hodgson, M.S. Kelly, M. Lehto, L.F. Thompson
Department of Physics, University of Shekeld, Shekeld S3 7RH, United Kingdom¹⁰

K.A. Holderbach, A. Bohrer, S. Brandt, C. G. Rupen, A. Misiejuk, G. P. Range, U. Sieler
Fachbereich Physik, Universitat Siegen, D-57068 Siegen, Germany¹⁶

G. Giannini, B. Gobbo
Dipartimento di Fisica, Universita di Trieste e INFN Sezione di Trieste, I-34127 Trieste, Italy

J. Putz, J. Rothberg, S. W. Asserbaech, R.W. Williams
Experimental Elementary Particle Physics, University of Washington, WA 98195 Seattle, U.S.A.

S.R. Armstrong, E. Charles, P. Elmer, D.P.S. Ferguson, Y. Gao, S. Gonzalez, T.C. Greening, O.J. Hayes,
H. Hu, S. Jin, P.A. McNamara III, J.M. Nachtman,² J. Nielsen, W. O. Rejidos, Y.B. Pan, Y. Saadi,
I.J. Scott, J. Walsh, Sau Lan Wu, X. Wu, G. Zobemig
Department of Physics, University of Wisconsin, Madison, WI 53706, USA¹¹

¹Also at CERN, 1211 Geneva 23, Switzerland.

²Now at University of California at Los Angeles (UCLA), Los Angeles, CA 90024, U.S.A.

³Also at Dipartimento di Fisica, INFN Sezione di Catania, 95129 Catania, Italy.

⁴Also Istituto di Fisica Generale, Universita di Torino, 10125 Torino, Italy.

⁵Also Istituto di Cosmologia e Geofisica del CNR, Torino, Italy.

⁶Supported by the Commission of the European Communities, contract ERBFMBICT982894.

⁷Supported by CICT, Spain.

⁸Supported by the National Science Foundation of China.

⁹Supported by the Danish Natural Science Research Council.

¹⁰Supported by the UK Particle Physics and Astronomy Research Council.

¹¹Supported by the US Department of Energy, grant DE-FG 0295-ER 40896.

¹²Now at LAL, 91898 Orsay, France.

¹³Supported by the US Department of Energy, contract DE-FG 05-92ER 40742.

¹⁴Supported by the US Department of Energy, contract DE-FC 05-85ER 250000.

¹⁵Permanent address: Universitat de Barcelona, 08208 Barcelona, Spain.

¹⁶Supported by the Bundesministerium für Bildung, Wissenschaft, Forschung und Technologie, Germany.

¹⁷Supported by the Direction des Sciences de la Matière, C.E.A.

¹⁸Supported by Fonds zur Förderung der wissenschaftlichen Forschung, Austria.

¹⁹Now at SAP AG, 69185 Walldorf, Germany

²⁰Now at Harvard University, Cambridge, MA 02138, U.S.A.

²¹Now at Département de Physique, Faculté des Sciences de Tunis, 1060 Le Belvedere, Tunisia.

²²Supported by the US Department of Energy, grant DE-FG 03-92ER 40689

1 Introduction

This letter presents results on W -pair production using data collected with the ALEPH detector at centre-of-mass energies ranging from 180.8 to 183.8 GeV, during the 1997 data taking period.

The experimental conditions and data analysis follow closely those used in the cross section measurement at lower LEP2 energies. As they are already described in detail in [1], attention will be focused on changes in selection procedures other than a simple rescaling of cuts with the increased collision energy.

At these energies the cross section has a much smaller dependence on the W mass with respect to the threshold productions, and the total production rate constitutes a test of the Standard Model (SM).

About 900 W pairs are expected in the collected data sample, allowing improved direct determinations of the W hadronic and leptonic branching ratios. The hadronic branching ratio is sensitive to the yet poorly known coupling \mathcal{V}_{csj} of the W to cs pairs.

A detailed description of the ALEPH detector can be found in Ref. [2] and of its performance in Ref. [3]. The luminosity is measured with small-angle Bhabha events, using lead-proportional wire sampling calorimeters [4], with an accepted Bhabha cross section of approximately 4.6 nb [5]. An integrated luminosity of 56.81 ± 0.11 (stat.) ± 0.29 (syst.) pb^{-1} was recorded, at a mean centre-of-mass energy of 182.66 ± 0.05 GeV [6].

2 Physics processes and definition of the W -pair cross section

To lowest order within the Standard Model, three diagrams contribute to W -pair production in e^+e^- annihilations: the s -channel γ and Z boson exchange and the t -channel e exchange, referred to as CC03 diagrams. Each W is expected to decay rapidly into a quark-antiquark pair ($W \rightarrow \bar{u}d; \bar{c}d; \bar{u}s; \bar{c}s; \bar{u}b; \bar{c}b$) or a lepton-neutrino pair ($W \rightarrow e^- \bar{\nu}_e; \mu^- \bar{\nu}_\mu; \tau^- \bar{\nu}_\tau$). Therefore, each CC03 diagram leads to an experimentally accessible four-fermion final state. However, many other Standard Model processes can lead to the same four-fermion final states as W -pair decays, interfering with the CC03 diagrams.

In the following, all signal cross sections are defined by the production of four-fermion final states only through two resonating W bosons, and will be referred as CC03 cross sections. The effect of the non-CC03 diagrams is corrected for with additive terms, obtained by comparing Monte Carlo (MC) simulations including only CC03 processes with all Standard Model four-fermion final states compatible with W -pair decays (W -like four-fermion final states), following the same procedure as in Ref. [1]. Such Monte Carlo additive terms are referred to in the following as "4f-CC03 corrections". They are computed separately for all different W -like four-fermion final states $f_1 f_2 f_3 f_4$, as $(\sigma_{4f} - \sigma_{CC03})_{f_1 f_2 f_3 f_4}$, where σ_{4f} and σ_{CC03} refer to MC selection efficiencies and generator cross sections, on samples of $f_1 f_2 f_3 f_4$ final states generated with the full four-fermion productions (4f subscript) or with W -pair decays only (CC03 subscript). All the signal

efficiencies quoted in the following are to be interpreted as CC03 efficiencies, evaluated on such Monte Carlo samples.

Two Monte Carlo event generators are used to simulate the signal events. Samples of events are generated with different W masses, both for CC03 diagrams and for all WW -like four-fermion diagrams, with KORALW [7]. A comparison sample is generated with EXCALIBUR [8] with and without colour reconnection effects (following the ansatz of Ref. [9]). The KORALW samples serve to determine the four-fermion and CC03 efficiencies used to obtain the final result. Other KORALW samples are used to check the m_W dependence of the selection procedures and of the four-fermion to CC03 correction. The EXCALIBUR samples are used as a check of the Monte Carlo simulation of the physics processes, and to assess the effects of colour reconnection.

The PYTHIA 5.7 [10] Monte Carlo program is used to generate background events coming from qq , ZZ , Zee and $W e$ processes. Other background events are generated with PHOT02 [11] for gamma-gamma interactions, KORALZ [12] for e^+e^- pair production, BHWIDE [13] and UNIBAB [14] for Bhabha scattering events. For the fully leptonic selections, non- WW -like four-fermion background processes with two visible leptons (as e^+e^- , $\mu^+\mu^-$, $e^+\mu^-$, $e^-\mu^+$) are generated with EXCALIBUR. Care is taken to avoid double counting of backgrounds with different generators and to avoid counting as backgrounds those WW -like four-fermion processes that are part of the 4f-CC03 correction. Monte Carlo samples corresponding to integrated luminosities at least twenty times as large as that of the data are fully simulated for all background reactions.

3 Selection of W -pair candidates

3.1 $WW \rightarrow \ell\ell$ events

The selection of fully leptonic W -pair decays is an update of the two selections used for the cross section and branching ratio measurements at 161 and 172 GeV [1], to the 183 GeV energy regime.

In the first selection, which does not make use of lepton identification criteria, two changes are introduced. The lepton-lepton acoplanarity is required to be smaller than 175 and the energy of the leading lepton must be smaller than 86 GeV. In the data, 47 events are selected with this analysis.

In the second selection lepton identification is used to classify events in six different di-lepton channels (ee , $e\mu$, $e\tau$, $\mu\mu$, $\mu\tau$ or $\tau\tau$), according to the flavour of leptons, and optimised cuts are applied individually in each channel. The electron and muon identification criteria are the same as those used for the leptonic classifications at lower energies [1]. A lepton then is classified as a tau either if no lepton identification is fulfilled or if the identified lepton has an energy lower than 25 GeV ($0.137 \frac{m_{\tau^0}}{s}$). In the data, 57 events are selected with this second analysis.

The inclusive combination of the two selections has an efficiency of 71.5% for the fully leptonic WW channels, combined assuming lepton universality. For the cross sections and the branching ratio measurements, the events selected by the combination of the two analyses are classified into six channels according to the di-lepton flavour classification used for the second selection. The CC03 efficiencies in the individual $\ell\ell$ channels are

given in Table 1 for the inclusive combination of the two selections. The total background amounts to 151 fb and is dominated by W^+W^- and non- W^+W^- -like four-fermion events, as $e^+e^- \rightarrow \nu\bar{\nu} \gamma \gamma$ with $\nu \in \mu, \tau$. In the data, the inclusive combination selects 61 events.

Table 1: Summary of results of the different event selections on Monte Carlo and Data events. Efficiencies are given in percent of CC03 processes. The qq selection column refers to the performance of the exclusive selection. The $qqqq$ column refers to events with a NN output greater than -0.2 . The listed backgrounds do not include the 4fCC03 corrections. In the $qqqq$ column the backgrounds include non- $qqqq$ W^+W^- decays.

		Event selection and classification										
		e^+e^-	$e^+e^-e^-$	$e^+e^-e^+$	$e^+e^-e^-e^+$	$e^+e^-e^-e^-$	$e^+e^-e^-e^+$	$e^+e^-e^-e^-$	e^+e^-qq	qq	qq	$qqqq$
Eff. for W^+W^- (in %)	e^+e^-	68.2	-	8.4	-	-	-	-	-	-	-	76.6
	e^-	0.1	70.8	2.0	-	2.9	0.3	-	-	-	-	76.1
	e^+	4.3	3.8	57.9	-	0.1	3.5	0.3	-	-	-	69.9
	W^+W^-	-	-	-	71.1	4.7	0.2	-	-	-	-	76.0
	W^+W^-	-	4.1	0.2	3.9	61.7	1.5	-	0.6	-	-	72.0
	W^+W^-	-	0.7	5.1	0.3	5.6	45.2	-	-	-	-	56.9
	e^+qq	-	-	-	-	-	-	81.2	0.3	6.2	-	87.7
	qq	-	-	-	-	-	-	0.2	88.6	3.5	-	92.3
qq	-	-	-	-	-	-	3.1	3.3	54.1	-	60.5	
$qqqq$	-	-	-	-	-	-	0.1	-	0.1	84.3	84.5	
Backgrounds (in pb)		0.02	0.01	0.05	0.01	0.02	0.05	0.11	0.05	0.11	1.24	1.67
Observed Events		6	14	18	8	11	4	127	113	86	432	818

All

Beam related background and detector noise are not fully reproduced by the simulation and affect the efficiency of the photon veto cuts. Random trigger events are used to compute the inefficiency introduced. The result is $(4.3 \pm 0.8)\%$ for the low angle photon veto and is applied as a correction factor lowering the Monte Carlo efficiencies. The systematic error takes into account the uncertainty on the inefficiencies. For the large angle photon veto these effects are not corrected for, but a systematic error of 1.7% is assigned to them, again from the study of random trigger events. Lepton identification efficiency has a 2% systematic uncertainty, to cover residual discrepancies in identification efficiency and purity between LEP1 data and Monte Carlo. The main sources of systematic errors are listed Table 2. The effect on the total cross section amounts to 0.04 pb and is dominated by the Monte Carlo statistical errors in the subtraction of backgrounds and in the signal efficiencies.

A likelihood fit is applied to determine individual cross sections for each fully leptonic decay channel using efficiency matrices for CC03 and backgrounds, as in Table 1. W^+W^- -like four-fermion processes are taken into account in the 4fCC03 correction for each individual channel, given by $(\sigma_{4f} - \sigma_{CC03}) / \sigma_{CC03}$. For all channels together, this correction

Table 2: Systematic errors summary in fb.

Source	W W cross section		
	$\ell\ell$	ℓqq	$qqqq$
Calibration of calorimeters			10
Preselection and Shape variables			155
W W generator and m_W dependence			105
W W fragmentation			60
QCD generator			60
Final State Interactions			40
Background normalisation	17	80	120
Luminosity	9	40	50
MC statistics	28	54	20
Photon veto	23	70	
Lepton id	5	30	
Lepton isolation		40	
Probability discrimination		40	
Total	41	141	247

amounts to $+6.19$ fb, where the uncertainty comes from Monte Carlo statistics.

The results of the fit, where the cross sections are constrained to be positive, yield

$$\begin{aligned}
 (W W \rightarrow e e) &= 0.12_{-0.06}^{+0.08} \text{ (stat.) } 0.01 \text{ (syst.) pb;} \\
 (W W \rightarrow \mu \mu) &= 0.17_{-0.07}^{+0.08} \text{ (stat.) } 0.01 \text{ (syst.) pb;} \\
 (W W \rightarrow \tau \tau) &= 0.00_{-0.00}^{+0.08} \text{ (stat.) } 0.03 \text{ (syst.) pb;} \\
 (W W \rightarrow e \mu) &= 0.33_{-0.09}^{+0.11} \text{ (stat.) } 0.02 \text{ (syst.) pb;} \\
 (W W \rightarrow e \tau) &= 0.44_{-0.12}^{+0.15} \text{ (stat.) } 0.03 \text{ (syst.) pb;} \\
 (W W \rightarrow \mu \tau) &= 0.27_{-0.09}^{+0.11} \text{ (stat.) } 0.02 \text{ (syst.) pb;}
 \end{aligned}$$

where the statistical errors correspond to a variation of the likelihood logarithm of 0.5 around the fitted maximum. The systematic errors are obtained by varying all input parameters in the fit according to their uncertainties. For $(W W \rightarrow \tau \tau)$, the systematic uncertainty refers to the positive statistical error, rather than to the fitted central value.

The fully leptonic cross section is obtained with the same fit, assuming lepton universality, and yields

$$(W W \rightarrow \ell \ell) = 1.38 \pm 0.20 \text{ (stat.) } 0.04 \text{ (syst.) pb.}$$

3.2 $W W \rightarrow \ell qq$ events

The three selection procedures developed for the lower energy measurements are applied. One selection is optimised for $W W$ events with electrons or muons and requires an energetic identified electron or muon, while the other two are designed for ℓqq events, based on global variables and topological properties of events.

3.2.1 $W W \rightarrow e q \bar{q}$ and $W W \rightarrow \mu q \bar{q}$ selections

The selection of $e q \bar{q}$ and $\mu q \bar{q}$ events is basically unchanged with respect to the previous analysis [1]. After the preselection of hadronic events based on charged energy and multiplicity, the charged track with the highest momentum component antiparallel to the missing momentum is chosen as the lepton candidate. The same electron or muon identification criteria as for the fully leptonic channel are required for this lepton candidate track, as well as an energy of at least 15 GeV. The probability for an event to come from a signal process is determined from the energy and isolation of the lepton and the total missing transverse momentum. Selected events are required to have a probability greater than 0.55, both for electron and muon candidates (Fig. 1).

The CC03 selection efficiencies are 81.5% for the $e q \bar{q}$ and 88.8% for the $\mu q \bar{q}$ channel, with a total background of 158 fb; 127 electron and 113 muon events are selected in the data.

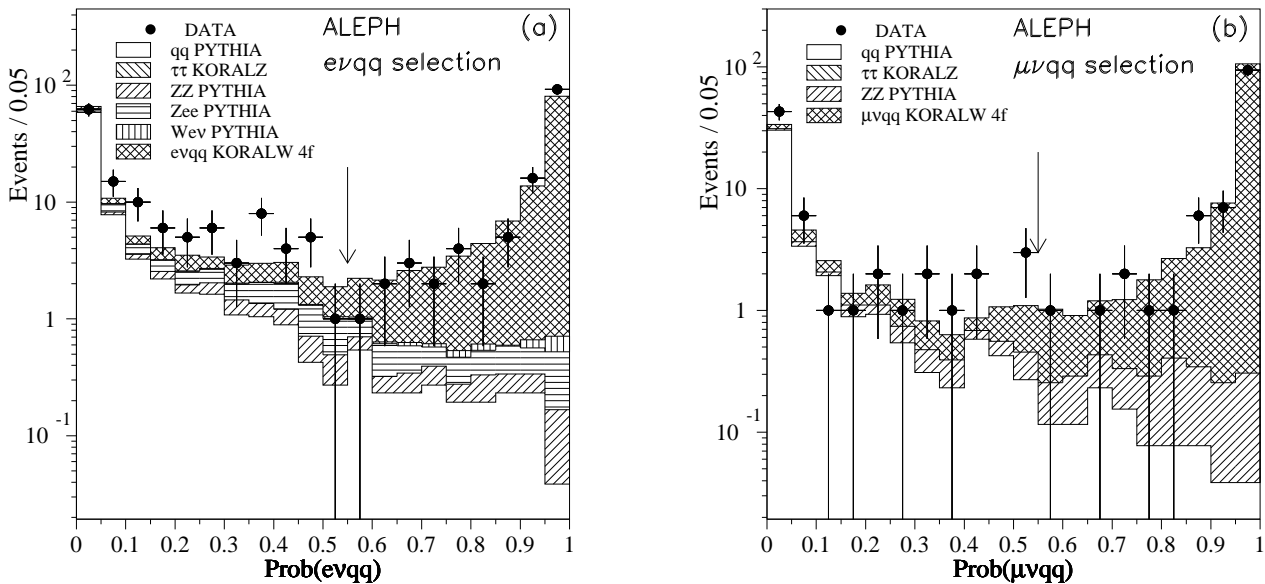


Figure 1: Probability distribution of preselected events for the $e q \bar{q}$ (a) and the $\mu q \bar{q}$ (b) selections. The arrows show the cuts above which events are kept in the selection.

3.2.2 $W W \rightarrow \mu q \bar{q}$ events

The selection of $\mu q \bar{q}$ events is based on global event variables and is combined with a topological selection designed to identify the μ jet. The common preselection is described in Ref. [1]. In the global analysis the acoplanarity is required to be less than 175, the energy in a wedge of half-angle 30 centred on the missing momentum direction in the plane transverse to the beam axis smaller than $12.5\% \sqrt{s}$, the estimated energy of the "primary" neutrino smaller than 65 GeV, and the visible mass smaller than $140 \text{ GeV} = c^2$. In the topological analysis the higher energy of the two quark jets must be smaller than 65 GeV and the acolinearity of the quark jets more than 110.

In the data 238 events are selected by the combined analyses, of which 152 are already in the e - qq and μ - qq samples. The tau exclusive selection, i.e. not counting events already selected by the electron and muon semileptonic selections, has an efficiency of 54.1% and total background of 114 fb, dominated by qq events.

3.2.3 Results

The inclusive combined efficiencies for the three semileptonic decay channels are 87.7% for the electron channel, 92.3% for the muon channel and 60.5% for the tau channel, giving an 80.2% overall efficiency for $WW \rightarrow \ell\ell qq$, with a background of 270 fb (Table 1). The overall 4fCC03 correction is +35–36 fb. A total of 322 events are selected in the data.

The systematic uncertainties on the cross sections (Table 2) are dominated by the background normalisation, and by the uncertainty coming from the cut on energy around the beam for qq events. Since the selections of semileptonic events is basically unchanged, all systematic uncertainties on the signal efficiencies and on the backgrounds have been evaluated in the same way as for the lower energy measurements [1].

A similar fit as for fully leptonic events is used here with the corresponding matrix of efficiencies and backgrounds including the overlaps of the different $\ell\ell qq$ analyses. The partial cross sections are then extracted from such a maximum likelihood fit to the number of events in each selection, leading to

$$\begin{aligned} \sigma(WW \rightarrow e qq) &= 2.52 \pm 0.24 \text{ (stat.)} \pm 0.06 \text{ (syst.) pb;} \\ \sigma(WW \rightarrow \mu qq) &= 2.12 \pm 0.21 \text{ (stat.)} \pm 0.06 \text{ (syst.) pb;} \\ \sigma(WW \rightarrow \tau qq) &= 2.15 \pm 0.31 \text{ (stat.)} \pm 0.09 \text{ (syst.) pb;} \end{aligned}$$

where the systematic errors are obtained by varying all input parameters of the fit according to their uncertainties.

The total $\ell\ell qq$ cross section is extracted by means of the same fit, under the assumption of lepton universality:

$$\sigma(WW \rightarrow \ell\ell qq) = 6.81 \pm 0.40 \text{ (stat.)} \pm 0.14 \text{ (syst.) pb.}$$

3.3 $WW \rightarrow qqqq$ events

The analysis of WW decays to four jets is updated from Ref. [1] and consists of a simple preselection followed by a fit to the distribution of the output of a neural net (NN).

For each event, particles are clustered into four jets with the DURHAM algorithm [15]. A first preselection cut rejects events with a real Z and large undetected initial state radiation, requiring that the total longitudinal momentum be smaller than 95% of the difference between the visible mass and the mass of the Z . The sphericity must be larger than 0.03. The value Y_{34} of the jet resolution parameter where a four jet becomes a three jet event, is required to be greater than 0.001. A further requirement that none of the four jets contains more than 95% of electromagnetic energy rejects qq events with a visible initial state radiation photon.

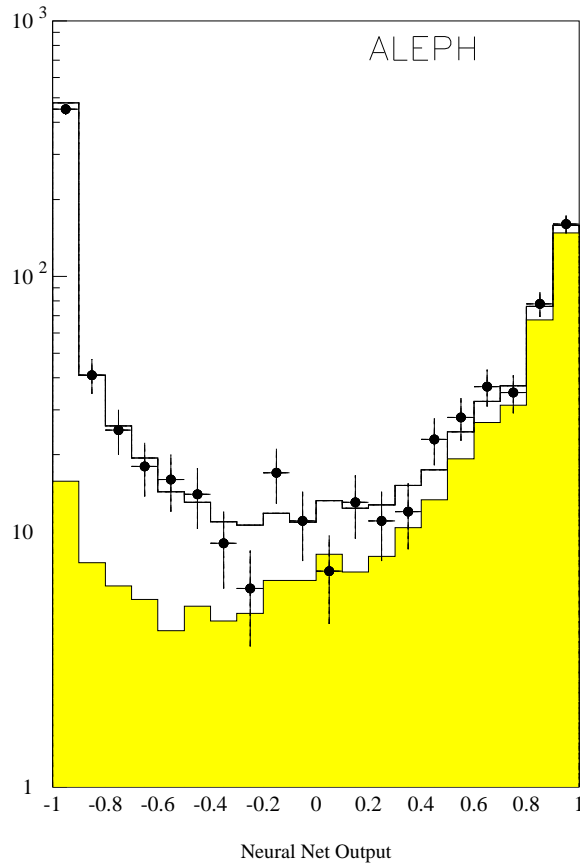


Figure 2: Comparison of NN output distributions for data and Monte Carlo after the preselection. The points are the data and the open histogram the total Monte Carlo prediction. The light shaded histogram shows the expected $W W + q q q q$ contribution.

At this level of the selection, 1014 events are selected in the data while 995.4 events are expected from all Standard Model processes. This preselection has an efficiency of 97% on CC03 events and a purity of 40%.

The input variables for the NN are described in Appendix A, and are related to the global event properties, the properties of jets, $W W$ kinematics and the b -tag probabilities for the four jets. Figure 2 gives the distribution of the NN output values for all backgrounds and signal Monte Carlo events compared with the data.

The number of signal events is extracted by means of a binned maximum likelihood fit to the distribution of the NN output for data events. Only the normalisation of the MC signal is allowed to vary in the fit. The 4fCC03 correction is +10.8fb.

The fit result is

$$(W W + q q q q) = 7.35 \pm 0.42 \text{ (stat.)} \pm 0.25 \text{ (syst.) pb:}$$

Systematic errors are summarised in Table 2. The uncertainty on the variables used for the event preselection cuts, and for the NN input (preselection and shape variables), has been assessed by reweighting the events in the NN output according to bin by bin Data/MC differences in the distributions of such variables. Uncertainties with the

WW generator have been evaluated comparing KORALW and EXCALIBUR MC samples, EXCALIBUR has also been used to evaluate the effects of colour reconnection. Finally, for the QCD fragmentation uncertainty, the HERWIG [16] generator was used to produce different samples of WW signal and qq background events.

4 Total cross section

The total cross section is obtained from a fit assuming the Standard Model branching ratios, the only unknown being the total cross section. The fit is applied to all data selected as described in the previous sections, and using the matrices of efficiencies and backgrounds of the various analyses, yielding

$$\sigma_{WW} = 15.57 \pm 0.62 \text{ (stat.)} \pm 0.29 \text{ (syst.) pb}$$

Figure 3 shows the total cross section measured as a function of the cm energy.

5 Branching ratios and V_{CS}

The same fit as for the total cross section is performed adding together the data samples collected at 161, 172 and 183 GeV centre-of-mass energies.

Without assuming lepton coupling universality, the six unknowns are the three individual leptonic branching ratios and the three total cross sections at 161, 172 and 183 GeV. The hadronic branching ratio is set to $1 - B_e - B_\mu - B_\tau$. The fitted leptonic branching ratios are

$$\begin{aligned} B(W \rightarrow e) &= 11.15 \pm 0.85 \text{ (stat.)} \pm 0.24 \text{ (syst.)} \% ; \\ B(W \rightarrow \mu) &= 10.06 \pm 0.78 \text{ (stat.)} \pm 0.21 \text{ (syst.)} \% ; \\ B(W \rightarrow \tau) &= 9.76 \pm 1.01 \text{ (stat.)} \pm 0.33 \text{ (syst.)} \% ; \end{aligned}$$

and are consistent with lepton universality and the Standard Model expectations. Due to cross-contaminations in the identification of W decays to μ versus e or τ , the measured $B(W \rightarrow \mu)$ is 26% anticorrelated with $B(W \rightarrow e)$ and 22% anticorrelated with $B(W \rightarrow \tau)$.

If lepton universality is assumed ($B_e = B_\mu = B_\tau = (1 - B_q)/3$), a fit to $B(W \rightarrow qq)$ and the three total cross sections as unknowns yields the measurement of the hadronic branching ratio

$$B(W \rightarrow qq) = 68.93 \pm 1.21 \text{ (stat.)} \pm 0.51 \text{ (syst.)} \% :$$

This result can be expressed in terms of the individual couplings of the W to quark-antiquark pairs:

$$\frac{B(W \rightarrow qq)}{1 - B(W \rightarrow qq)} = (\mathcal{V}_{ud}^2 + \mathcal{V}_{cd}^2 + \mathcal{V}_{us}^2 + \mathcal{V}_{cs}^2 + \mathcal{V}_{ub}^2 + \mathcal{V}_{cb}^2) (1 + s_W^2(m_W^2)) = \quad (1)$$

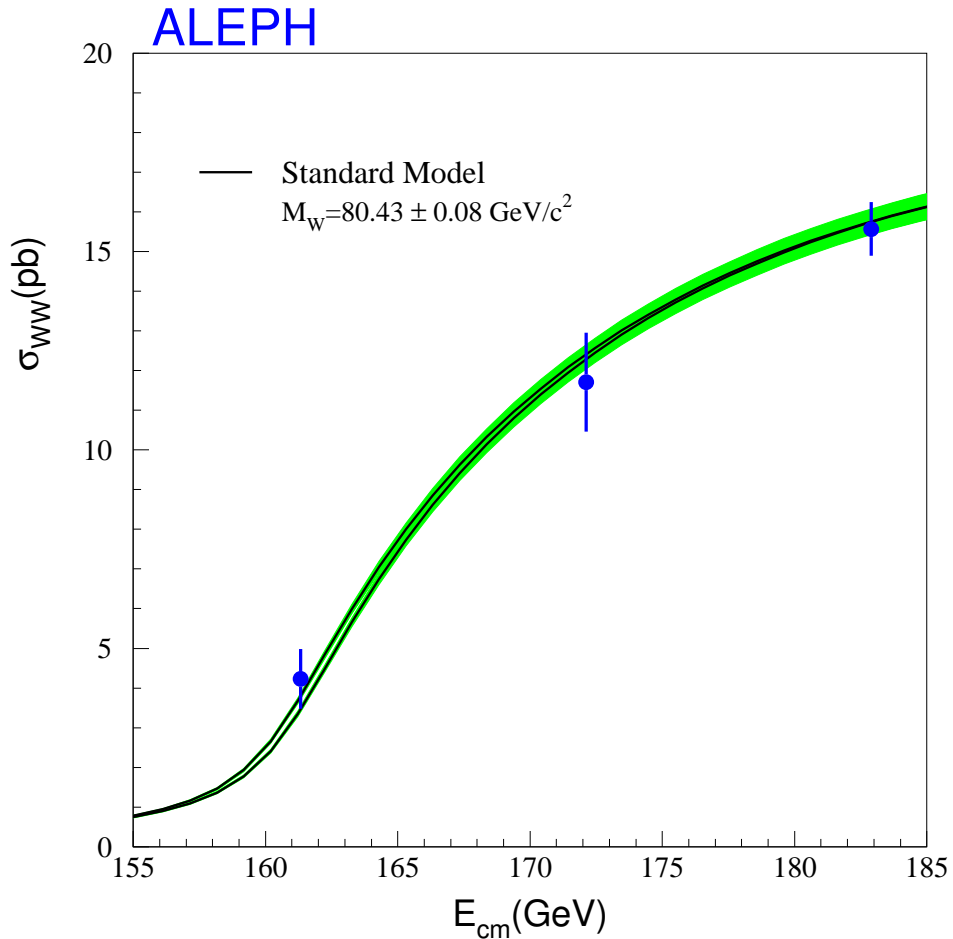


Figure 3: Measurements of the W -pair production cross section at three centre-of-mass energies, compared to the Standard Model prediction from GENTLE [18] for the world average value of the W mass [19]. The two curves correspond to the $80 \text{ MeV}/c^2$ error on m_W , the shaded area around the two curves represents the theoretical error (2%) on the GENTLE calculations.

Using the world average value of $|V_{cs}|$ (m_Z^2) evolved to m_W^2 together with the other measured CKM matrix elements [17] allows a constraint on the least well measured CKM matrix element,

$$|V_{cs}| = 1.043 \pm 0.058 (\text{stat.}) \pm 0.026 (\text{syst.})$$

6 Invisible W width

The cross section given in the previous sections are based on the assumption that the W decays exclusively into the known quarks and leptons. Scenarios of new physics have been advocated whereby the W could decay into a charged particle with momentum below detectability, $P < 200 \text{ MeV} = c$ [20]. These decays would appear as invisible, in that events containing them would not be selected by the previously described selections. A first consequence would be the appearance of events with only one visible W decay. A direct search for this scenario has been performed by ALEPH and is described elsewhere [21].

A second consequence would be a modification of the visible W cross section as follows. The total width Γ_W of the W boson would be increased with respect to the Standard Model prediction for decays into known fermions, Γ_W^{vis} , by the corresponding invisible partial width,

$$\Gamma_W = \Gamma_W^{\text{vis}} + \Gamma_W^{\text{invis}};$$

The dominant effect would be a decrease of the visible cross section σ_{WW}^{vis} according to

$$\sigma_{WW}^{\text{vis}} = (B^{\text{vis}})^2 \sigma_{WW};$$

where

$$B^{\text{vis}} = \frac{\Gamma_W^{\text{vis}}}{\Gamma_W^{\text{vis}} + \Gamma_W^{\text{invis}}} = 1 - B^{\text{invis}};$$

The total cross section σ_{WW} has a non-negligible, but small, dependence upon a change of the total width, if one assumes that the couplings of the W to known fermions are left unmodified. The above formulae have to be corrected for mixed decays, in which one W boson decays to a visible channel while the other W boson decay is undetected. These events would not be completely missed by the standard analyses, they have an efficiency to be selected by the qq selection of 22.4% and 8.9% at 172 and 183 GeV, respectively. Such events would not be detected by the other selections. This correction term is proportional to $\frac{\Gamma_W^{\text{invis}}}{\Gamma_W} = \frac{\Gamma_W^{\text{vis}}}{\Gamma_W}$ and the above selection efficiency; it represents a change in the visible cross section at the permil level.

The invisible width Γ_W^{invis} is extracted by means of a fit to the measured cross sections at $\sqrt{s} = 161, 172$ and 183 GeV , taking into account common systematic errors in the theoretical prediction and in the event selection. The theoretical prediction of σ_{WW} is computed with GENTLE [18], taking into account its residual sensitivity to a change in the total width. The possibility that the triple gauge boson couplings could be anomalous is allowed, by fitting simultaneously κ ; and g_1^Z within the constraints allowed by the analysis of angular distributions in the semileptonic channel [22]. The W mass is allowed to vary in the fit within the constraint imposed by the current world average value (not including the W mass from the WW cross section measurements at LEP), $m_W = 80.43 \pm 0.08 \text{ GeV} = c^2$ [19].

In addition to the systematic errors on the cross section measurements, three more correlated systematic errors are considered: i) a theoretical uncertainty of 2% in the prediction of the total WW cross section, ii) a theoretical uncertainty of 0.5% in the Standard Model W width and iii) the beam energy uncertainty $E_b = 25 \text{ MeV}$, where the last two sources of systematic uncertainty have been found to have a negligible effect

(below 1 M eV). The different contributions to the total systematic error are summarized in Table 3.

The fit to the cross section data [1] gives

$$\begin{aligned} \sigma_W^{\text{invis}} &= 30^{+52}_{-48} \text{ (stat.) } 33 \text{ (syst.) M eV}^2 \text{ (} \chi^2/\text{dof} = 3.5=2); \\ \sigma_W^{\text{invis}} &< 139 \text{ M eV}^2 \text{ at 95\% C.L.}; \\ B_W^{\text{invis}} &< 6.5\% \text{ at 95\% C.L.} \end{aligned}$$

The corresponding total W width is

$$\Gamma_W = 2.126^{+0.052}_{-0.048} \text{ (stat.) } 0.035 \text{ (syst.) G eV}.$$

Table 3: Summary of systematic uncertainties on the σ_W^{invis} determination from the cross section measurement.

Source	σ_W^{invis} [M eV ²]
Cross section measurement	24
Theor. uncertainty on Γ_W	23
Total uncertainty	33

7 Conclusions

Using an integrated luminosity of 57 pb⁻¹ the W pair production cross section at $\sqrt{s} = 182.7$ GeV has been measured in all decay channels. The determination of individual branching ratios has been performed. The total cross section is 15.57 ± 0.62 (stat.) ± 0.29 (syst.) pb. After adding the data taken at 161 and 172 GeV c.m. energy, the hadronic decay branching ratio is 68.93 ± 1.21 (stat.) ± 0.51 (syst.)% which is used to determine the CKM matrix element $|V_{cs}| = 1.043 ± 0.058$ (stat.) ± 0.026 (syst.). These results are consistent with similar measurements performed at LEP at the same centre-of-mass energy [23].

The agreement of the cross section with the Standard Model prediction allows a limit to be set on the W partial width into invisible decays: $\sigma_W^{\text{invis}} = 30^{+52}_{-48}$ (stat.) 33 (syst.) M eV², $B_W^{\text{invis}} < 139$ M eV² at 95% C.L.:

Acknowledgements

It is a pleasure to congratulate our colleagues from the CERN accelerator divisions for the successful operation of LEP at 183 GeV. We are indebted to the engineers and technicians in all our institutions for their contributions to the excellent performance of ALEPH. Those of us from non-member countries thank CERN for its hospitality.

Appendix A . Hadronic neural network input variables

The neural network hadronic event selection uses 19 variables. These are based on global event properties, heavy quark flavour tagging, jet properties and WW kinematics and are listed below together with their discriminating power. The four jets are numbered in order of decreasing energy.

Global event properties

Fox Wolfram moment H0 (4.4%)

Fox Wolfram moment H2 (4.7%)

Fox Wolfram moment H4 (10.1%)

Sphericity (3.9%)

Missing Energy (4.4%)

Sum of the p_t^2 of all charged tracks to the beam axis (4.1%)

Heavy flavour tagging

Sum of the b-tag probabilities for the four jets (5.7%)

The following jet related variables are determined from kinematically fitted jet momenta.

Jet properties

Number of good charged tracks in jet1 (6.2%)

Maximum energy carried by one energy flow particle in Jet1 (3.8%)

Maximum energy carried by one energy flow particle in Jet2 (4.6%)

Maximum energy carried by one energy flow particle in Jet3 (4.7%)

Sum of the angles between the leading and remaining charged tracks in jet1 (5.5%)

Sum of the angles between the leading and remaining charged tracks in jet2 (3.6%)

WW kinematics

Sum of the cosines of the 6 angles between jets (8.7%)

Cosine of the angle between jet2 and jet3 (4.6%)

Energy of jet1 (8.1%)

Energy of jet2 (3.8%)

Momentum of jet4 (5.5%)

A symmetry in momentum between jet2 and jet3 (3.8%)

References

- [1] ALEPH Collaboration, Measurement of the W mass in e^+e^- collisions at production threshold, Phys. Lett. B 401 (1997) 347; ALEPH Collaboration, Measurement of W pair cross section in e^+e^- collisions at 172 GeV, Phys. Lett. B 415 (1997) 435.
- [2] ALEPH Collaboration, ALEPH: A detector for electron-positron annihilations at LEP, Nucl. Inst. Meth. A 294 (1990) 121.
- [3] ALEPH Collaboration, Performance of the ALEPH detector at LEP, Nucl. Inst. Meth. A 360 (1995) 481.
- [4] ALEPH Collaboration, Measurement of the absolute luminosity with the ALEPH detector, Z. Phys. C 53 (1992) 375.
- [5] BHLUMI, version 2.01, S. Jadach et al., Phys. Lett. B 253 (1991) 469; Phys. Lett. B 257 (1991) 173; Phys. Lett. B 260 (1991) 438; Comp. Phys. Commun. 70 (1992) 305.
- [6] The LEP Energy Working group, Evaluation of the LEP Centre-of-Mass Energy Above the W Pair Production Threshold, CERN-EP/98-191 (1998), submitted to Eur. Phys. J. C.
- [7] M. Skrzypek, S. Jadach, W. Placzek and Z. Was, Comp. Phys. Commun. 94 (1996) 216.
- [8] F. A. Berends, R. Pittau and R. Kleiss, Comp. Phys. Commun. 85 (1995) 437.
- [9] T. Sjöstrand and V. A. Khoze, Z. Phys. C 62 (1994) 281.
- [10] T. Sjöstrand, Comp. Phys. Commun. 82 (1994) 74.
- [11] ALEPH Collaboration, An experimental study of τ hadrons at LEP, Phys. Lett. B 313 (1993) 509.
- [12] S. Jadach, B. F. L. Ward and Z. Was, Comp. Phys. Commun. 79 (1994) 503.
- [13] S. Jadach et al., Phys. Lett. B 390 (1997) 298.
- [14] H. Anlauf et al., Comp. Phys. Commun. 79 (1994) 466.
- [15] Yu. L. Dokshitzer, J. Phys. G 17 (1991) 1441.
- [16] G. M. Archesini et al., Comp. Phys. Commun. 67 (1992) 465.
- [17] C. Caso et al. (Particle Data Group), Review of Particle Physics, Eur. Phys. J. C 3 (1998) 1.
- [18] D. Bardin et al., Nucl. Phys. (Proc. Suppl.) B 37 (1994) 148; D. Bardin et al., GENTLE/4fan v. 2.0: A Program for the Semi-Analytic Calculation of Predictions for the Process $e^+e^- \rightarrow 4f$, DESY 96-233, hep-ph/9612409.

- [19] D.R. Ward, Tests of the Standard Model: W mass and W W Z Couplings, talk given at EPS-HEP 97, Jerusalem, 20 August 1997.
- [20] J. Kalinowski and P.M. Zerwas, Phys. Lett. B 400 (1997) 112.
- [21] ALEPH Collaboration, Search for Single W Production at LEP 2, ICHEP-98/904.
- [22] ALEPH Collaboration, Measurement of Triple Gauge-Boson Couplings at 172 GeV, Phys. Lett. B 422 (1998) 369.
- [23] L3 Collaboration, Measurement of W Pair Cross Sections in e^+e^- Interactions at $\sqrt{s} = 183$ GeV and W Decay Branching Fractions, Phys. Lett. B 436 (1998) 437; OPAL Collaboration, W^+W^- production and triple gauge boson couplings at LEP energies up to 183 GeV, CERN-EP/98-167 (1998), submitted to Eur. Phys. J.C.